Vacuum/volume 33/number 7/pages 397 to 406/1983
Printed in Great Britain

0042-207X/83$3.00+.00

Studies of photon induced gas desorption using synchrotron radiation

O Gröbner, A G Mathewson, H Störi* and P Strubin, *CERN, 1211 Geneva 23, Switzerland*
and
R Souchet, *LAL, Orsay, 91405 Orsay Cedex, France*

received 2 August 1982; in revised form 17 February 1983

In view of finalizing the design of the vacuum system of the Large Electron and Positron Storage Ring (LEP) we have studied synchrotron radiation induced neutral gas desorption. A 3 m section of an aluminium vacuum chamber has been exposed to the photon beam emerging from the electron storage ring DCI in Orsay, under conditions closely simulating the environment in a particle accelerator. In order of importance the gases desorbed were H_2, CO_2, CO and CH_4 with H_2O practically absent. Under the experimental conditions of an unbaked chamber and 11 mrad glancing incidence of the photons, the initial molecular desorption yields for these gases were typically 0.5, 8×10^{-2}, 2×10^{-2} and 8×10^{-3} molecules per photon respectively. These values could be reduced by about 1 to 2 orders of magnitude during continued photon exposure and in most cases without evidence that this 'beam cleaning action' would be limited. After exposure to air and pumpdown of the previously cleaned chamber, we observe a significant memory effect. The dependence of the photon desorption on the angle of incidence has been studied down to a glancing angle of 11 mrad showing a definite deviation from the previously assumed $1/\sin\phi$ scaling. The implications of the results in terms of the expected beam-gas lifetime in LEP are discussed.

Introduction

In the vacuum system of the Large Electron Positron (LEP)[1] storage ring the average pressure over the 27 km circumference must be such that up to 9.25 mA of electrons and positrons with energies between 20 and 100 GeV may be stored for the order of 20 h without undue loss from beam-residual gas interaction.

The interior wall of the Al alloy vacuum chamber is subjected to intense synchrotron radiation from the relativistic electrons and positrons, the photon spectrum extending to well above 1 MeV, resulting in desorption of neutral gas from the chamber surface. The installed pumping system must therefore cope with this additional gas load as well as the normal thermal outgassing of the chamber. Unfortunately, the knowledge available from existing storage rings is limited and does not really permit us to extrapolate with sufficient confidence to the conditions which will prevail in LEP.

The most important questions among many which have to be answered are the following:

which gases are desorbed and how much and how does this desorption evolve with time,

what will be the synchrotron radiation induced pressure rise per mA of stored beam ($\Delta P/I$) both initially and after a given exposure to synchrotron radiation, and how is it affected by baking the chamber.

what is the effect of varying the photon angle of incidence and what is the desorption rate at the 7 mrad glancing angle of incidence in LEP.

how does the desorption process depend on photon energy,

what will be the rate of decrease of the synchrotron radiation induced gas desorption, the so-called self-cleaning time, in LEP when operating at its lowest energy of 20 GeV.

At the photon energies encountered in LEP, scattering of the radiation on the wall of the vacuum chamber is very important. For example, between 300 and 400 keV up to 50% of the incident power is scattered at large angles. This scattered radiation traverses the vacuum chamber where it is again scattered, this process continuing until finally the radiation is absorbed in the walls or escapes from the vacuum chamber. The associated electrons also produce secondary electrons which in turn produce more secondaries. Because of these processes the interior of the vacuum chamber is filled with photons and electrons of various energies incident on the surface at all angles. For this reason laboratory measurements on small samples are of limited value since they do not reproduce the actual conditions in a closed vacuum chamber.

Using chambers installed in the main vacuum system of existing machines is in most cases very difficult because of practical

* Present address: Technische Universität Wien, A-1040 Vienna, Austria.

limitations or the impossibility of varying parameters like the angle of incidence. Thus the offer to use an existing synchrotron radiation light port on the electron positron storage ring (DCI) at the Laboratoire de l'Accélérateur Linéaire, Orsay, France, was gratefully accepted.

2. Review of synchrotron radiation properties

2.1. The photon flux. The quantum spectrum of synchrotron radiation is given by[2]:

$$\frac{d^2N}{d\varepsilon\, dt} = \frac{9\sqrt{3}}{8\pi}\frac{W}{\varepsilon_c^2}\int_x^\infty K_{5/3}(y)\, dy$$

$$= \frac{6.95\ 10^{13}}{E^2} I\rho \int_x^\infty K_{5/3}(y)\, dy \text{ photons s}^{-1}\text{ eV}^{-1}$$

where $x=\varepsilon/\varepsilon_c$, $\varepsilon_c = 3/2\hbar c(E/E_0)^3/\rho = 2.218\ 10^3\ E^3/\rho$ eV

$$W = \frac{4\pi}{3}\frac{r_e}{e}\frac{E^4}{E_0^3}\frac{I}{\rho} = 88.5\ E^4 I/\rho \text{ Watts}$$

is the total radiated energy and

ε_c is the so called critical photon energy, which divides the power spectrum into two equal parts
E_0 is the electron rest energy
r_e is the classical electron radius
ε is the photon energy in eV
I is the beam current in mA
E is the machine energy in GeV
ρ is the bending radius in metres.

The integral is taken over the modified Bessel function $K_{5/3}$.

The spectrum can be expressed in the following form

$$\frac{d^2N}{dx\, dt} = \frac{\sqrt{3}r_e}{e\hbar c} EI \int_0^\infty K_{5/3}(y)\, dy.$$

The number of photons contained in the spectral interval $(0, x)$ follows by integration of the spectrum. Defining

$$F(x) = \int_0^x \int_u^\infty K_{5/3}(y)\, dy\, du$$

the photon flux can be expressed as

$$\dot{N}(x) = \frac{\sqrt{3}r_e}{e\hbar c} F(x) EI.$$

The function $F(x)$ has been computed and is shown in Figure 1. For $x \to \infty$, $F(x)$ takes the value 5.23.

With the numerical constants put in the photon flux is

$$\dot{N}(x) = 1.54 \times 10^{17}\ F(x) EI \text{ photons s}^{-1}.$$

The linear photon flux density per unit length, ds, of bending magnet is obtained by dividing this expression by $2\pi\rho$

$$\frac{d\dot{N}(x)}{ds} = 2.45 \times 10^{16}\ F(x)\frac{IE}{\rho} \text{ photons s}^{-1}\text{ m}^{-1}.$$

The total photon flux is

$$\dot{N} = 8.08 \times 10^{17}\ IE \text{ photons s}^{-1}$$

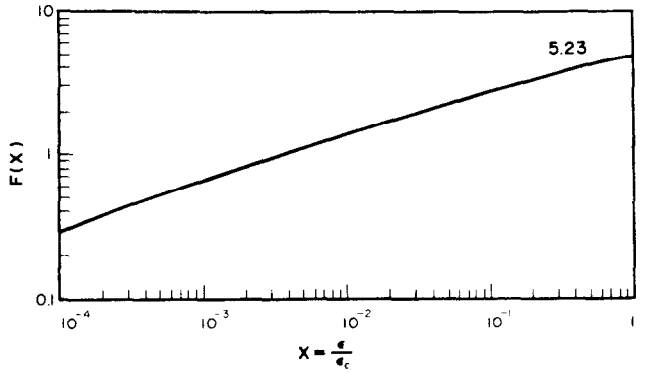

Figure 1. The function $F(x) = \int_0^x \int_u^\infty K_{5/3}(y)\, dy\, du$ as a function of $x = \varepsilon/\varepsilon_c$.

and the total photon flux per unit length is

$$\frac{d\dot{N}}{ds} = 1.28 \times 10^{17}\frac{IE}{\rho} \text{ photons s}^{-1}\text{ m}^{-1}.$$

2.2. Radiation power. The total power radiated by the DCI beam is given by the expression for W with $\rho = 3.82$ m. In the geometrical arrangement of the DCI radiation absorbers, the synchrotron radiation incident on the first collimator has a spread of about 17 mrad in the horizontal plane and 5 mrad (see section 4.1) in the vertical plane. In the collimator C_1 a square hole 13.4 × 13.4 mm limits the synchrotron radiation divergence to 5 mrad both horizontally and vertically.

The radiated power per radian in DCI is

$$W/2\pi = 3.68E^4 I \text{ Watts}.$$

At 1.72 GeV the radiated power per mA of circulating beam current falling on our test chamber amounts to 0.16 W per mA. The maximum current used in an experiment was 180 mA, giving about 30 W of total power. The power load on the first collimator is typically twice as large as on the chamber and therefore water cooling had to be provided.

3. Scaling between DCI and LEP

3.1. The critical energy. Since $\varepsilon_c = 2.218 \times 10^3\ E^3/\rho$ it follows that the critical energy scales like

$$\frac{\varepsilon_c(\text{LEP})}{\varepsilon_c(\text{DCI})} = \frac{\rho_{\text{DCI}}}{\rho_{\text{LEP}}}\left(\frac{E_{\text{LEP}}}{E_{\text{DCI}}}\right)^3.$$

Since the ratio of the bending radii in DCI and LEP is $3.82/3103.6 = 1.23 \times 10^{-3}$ the ratio of the machine energies which provides the same photon spectrum is 9.33. Hence the standard operating energy 1.72 GeV of DCI corresponds to 16 GeV in LEP which is only slightly less than the planned injection energy of 20 GeV.

3.2. The photon flux. The linear photon flux density scales like

$$\frac{(IE/\rho)_{\text{DCI}}}{(IE/\rho)_{\text{LEP}}}.$$

When operating at the same critical energy then the ratio of the

flux of photons per second and per metre of bending magnet is

$$\frac{\text{Flux (DCI)}}{\text{Flux (LEP}} = \frac{I_{\text{DCI}}}{L_{\text{LEP}}}\left(\frac{\rho_{\text{LEP}}}{\rho_{\text{DCI}}}\right)^{2/3} = 87.07\,\frac{I_{\text{DCI}}}{I_{\text{LEP}}}.$$

In the geometry which has been chosen for the DCI set-up, a 3.12 m long section of the test chamber receives photons emitted from an arc of 5×10^{-3} radians. The resulting photon flux per second and per metre of chamber is thus reduced by the geometrical factor f given by

$$f = \frac{5\times10^{-3}}{3.12}\rho_{\text{DCI}} = 6.1\times10^{-3}.$$

In our geometry we have therefore the scaling relation for the flux per metre

$$\frac{\text{Flux (DCI Test Chamber)}}{\text{Flux LEP}} = 0.53\,\frac{I_{\text{DCI}}}{I_{\text{LEP}}}.$$

Practical currents in DCI can be by as much as a factor of 50 larger than in LEP, producing a very intense photon flux. Due to this fact, it has been possible to study beam cleaning on a compressed time scale.

Since the injection energy in LEP will not be 16 but close to 20 GeV, the scaling factor decreases to 0.42. It follows that 1 mA in LEP is equivalent to about 2.5 mA for the DCI test chamber.

3.3. Relation between beam dose and the accumulated number of photons. The self-cleaning is commonly expressed as a function of the mA hours of machine operation. It has been shown that 1 mA in LEP gives the same photon flux per metre of chamber as 2.5 mA in DCI on our test chamber.

Alternatively, it may be desirable to express mA hours of circulating beam in terms of the photon flux per metre of test chamber. We find for 1.72 GeV beam energy that 1 mAh in DCI corresponds to a total of 1.3×10^{18} photons m^{-1}. This conversion factor has been used to transform the scales on the figures from beam dose to integrated photon flux.

3.4. Molecular desorption yield. From the specific pressure rise one can derive the molecular desorption yield η in molecules per photon through the relation

$$\frac{\Delta P}{I} = \eta\,\frac{\dot{N}/I}{CS}\ \text{torr mA}^{-1}$$

where $C = 3.2\times10^{19}$ molecules per torr l

S is the pumping speed determined by the known conductance to the test chamber (72.5 l s^{-1} for nitrogen).

$\Delta P/I$ is the pressure rise per mA of beam.

It must be noted that this definition of η in no way implies that the desorption of neutral gas is made directly by the photons. An intermediate step involving photoelectrons is by no means excluded but the two effects are difficult to separate in our experiment.

This equation can be rearranged to give the molecular desorption yield for the ith gas component of the total pressure increase

$$\eta_i = \frac{CS_i\,\Delta P_i/I}{\dot{N}/I}.$$

The pumping speed S_i scales with the molecular weight of the gas molecules m_i according to

$$S_i = 72.5\sqrt{28/m_i}\ \text{l s}^{-1}.$$

The total flux per mA of photons of all energies entering the test chamber in the chosen conditions of collimation of 5 mrad is

$$\frac{\dot{N}}{I} = \frac{5\times10^{-3}}{2\pi}\,8.05\times10^{17}\,E$$

$$= 6.41\times10^{14}E\ \text{photons s}^{-1}\ \text{mA}^{-1}$$

For η_i we find the expression

$$\eta_i = 1.92\times10^{7}\,\frac{\Delta P_i/I}{\sqrt{m_i E}}\ \text{molecules photon}^{-1}.$$

For $E = 1.72$ GeV the following relation between the specific pressure rise and the molecular desorption yield is obtained:

$$\eta_i = 1.11\times10^{7}\,\frac{\Delta P_i/I}{\sqrt{m_i}}\ \text{molecules photon}^{-1}.$$

In Table 1 are given the pumping speeds for the various gases and the conversion factors, k_i, from $\Delta P/I$ to η.

Table 1

m_i	S_i(l s^{-1})	k_i
2	271	7.9×10^{6}
16	96	2.8×10^{6}
18	90	2.6×10^{6}
28	72.5	2.1×10^{6}
44	58	1.7×10^{6}

4. Experimental set-up

4.1. Synchrotron light collimation. The synchrotron radiation light port on the bending magnet chamber in DCI provides for a horizontal opening angle of 16.7 mrad. However, in order to measure desorption at a glancing angle of incidence comparable to LEP, i.e. 6 mrad, a further collimation to 5 mrad has been introduced. This degree of collimation is a compromise between photon flux, spread in angle of incidence and the maximum use of the available space in the machine for mounting a long test chamber. The actual angle of incidence during the measurements was 11 mrad with a spread of ±2.5 mrad. Figure 2 illustrates the arrangement of collimators and chamber positions.

The angular spread $\Delta\psi$ (FWHM) out of the plane of the orbit of the beam for photon energies $\varepsilon \ll \varepsilon_c$ is[3]

$$\Delta\psi = \frac{2E_0}{E}\left(\frac{\varepsilon_c}{\varepsilon}\right)^{1/3}\ \text{rad}.$$

Since $\varepsilon_c \simeq E^3$ the spread $\Delta\psi$ is independent of the beam energy. One finds

$$\Delta\psi = 1.33\times10^{-2}(\rho\varepsilon)^{-1/3}\ \text{rad}.$$

We have chosen $\varepsilon = 5$ eV as the lower limit of the photon energy. This requires with $\rho = 3.82$ m an opening angle of 5 mrad for the vertical collimation.

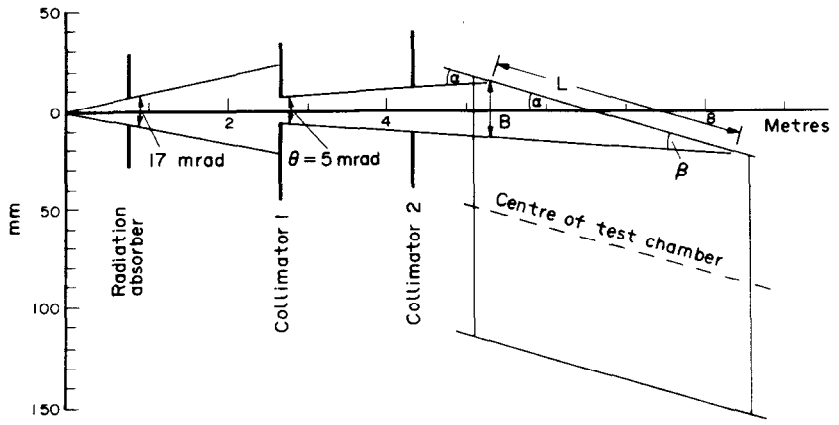

Figure 2. The position of the collimators and test chamber with respect to the source point of the synchrotron radiation. The angle of incidence $\alpha = 11$ mrad, β and $\gamma = \alpha \pm \theta/2$ and $\theta = 5$ mrad. The exposed length of the chamber $L = B/\beta = 3.12$ m.

The second collimator C_2 shown in Figure 2 having an opening of 25 x 25 mm has been chosen to serve as the known vacuum conductance necessary for quantitative desorption measurements and is not exposed to radiation.

4.2. Vacuum system. Figure 3 shows the layout of the vacuum system. Two straight-through valves were provided, a bakeable all metal sealed valve separating the experimental set-up from the DCI main ring vacuum system outside experimental runs and a second, viton sealed valve separating the aluminium test chamber from the differential pumping system. With this valve open the LEP test chamber was pumped via the 72.5 l s^{-1} (25 x 25 mm) conductance. The stainless steel pumping system consisted of a 400 l s^{-1} sputter ion pump and two Ti sublimation pumps providing a total pumping speed of at least 2000 l s^{-1} for CO which is much greater than the 72.5 l s^{-1} of the conductance. After a 12 h 300°C bakeout the pressure in this pumping system was $\sim 1 \times 10^{-10}$ torr.

The second straight through valve was used to separate the test chamber from the pumps during evacuation from atmospheric pressure and bakeouts when the test chamber was pumped by a turbomolecular pump. Thus ultra-high vacuum conditions could be maintained in the differential pumping system at all times no matter what the pressure in the test chamber.

Some hours before a measurement, the turbomolecular pump was valved off and the straight through valve opened. The nitrogen equivalent pressure in the pumping system stabilized at 8.8×10^{-10} torr giving $\sim 2.7 \times 10^{-8}$ torr in the unbaked test chamber. After baking the test chamber at 150°C for 12 h, the respective nitrogen equivalent pressures were 2.5×10^{-10} torr and 8.4×10^{-9} torr. The relatively high pressure in the test chamber after bakeout was due to the viton O-ring sealed valve which even after baking at 150°C for 12 h still had a high thermal outgassing rate, presumably from the viton and/or the internal bellows actuating mechanism which was impossible to bake above ~40°C.

Total pressure measurements in both the test chamber and the pumping system were made by calibrated Bayard–Alpert type gauges with X-ray limits $\sim 2 \times 10^{-11}$ torr. Partial pressure measurements in the test chamber were made with a quadrupole mass analyser calibrated against the total pressure gauge for the four gases H_2, CH_4, CO and CO_2. All partial pressures quoted in this report are absolute pressures.

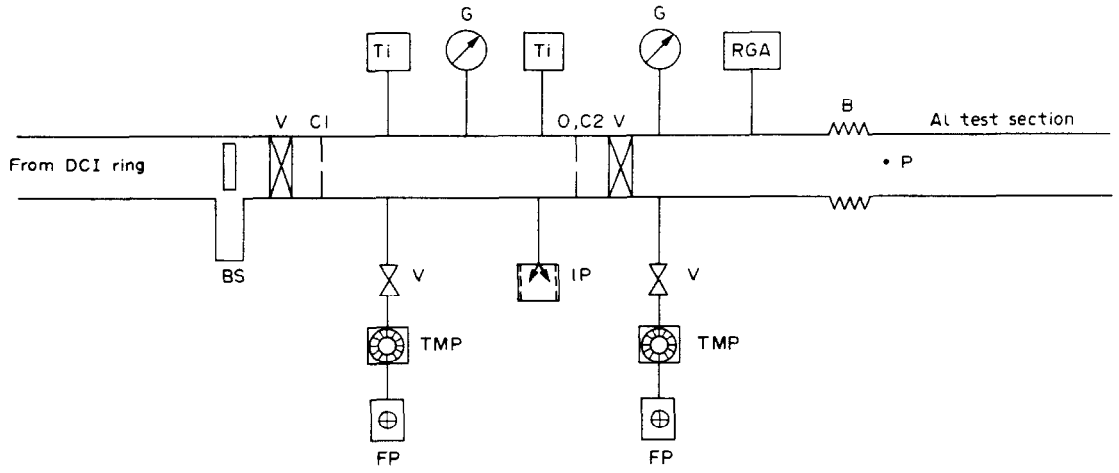

Figure 3. The layout of the vacuum system and test chamber. BS—beam stopper, V—uhv straight through valve, C_1—collimator, C_2—collimator and O—orifice (25 x 25 mm), B—bellows, P—pivot, G—vacuum gauge, RGA—residual gas analyser, Ti—titanium sublimation pump, IP—ion pump, TMP—turbomolecular pump, FP—fore pump.

The residual gas analyser was controlled by a microcomputer into which was also fed the total pressure in the test chamber and the DCI beam current. With such a system both total and partial pressure changes as a function of beam dose could be recorded every 30 s. In addition, time integration of the pressure was performed to give the total quantity of each gas species desorbed.

A remote-controlled water-cooled beam stopper was installed between the DCI machine and the first collimator. This enabled synchrotron radiation to be introduced into the test chamber or turned off at will thus the radiation dose seen by the test chamber could be well defined.

5. Results

5.1. The test chamber. The test chamber was manufactured from an extruded profile. The material was a precipitation hardenable alloy of the type ISO AlMgSi (composition Mg 0.35–0.6%, Si 0.3–0.6%, Fe 0.1–0.3%, Cu 0.1%, Mn 0.1%, Cr 0.05%, Zn 0.15%, Ti 0.1% Al-balance).

The chamber was chemically cleaned twice—once after all machining and again after all welding operations. The cleaning method consisted of vapour degreasing in perchloroethylene vapour at 121°C followed by ultrasonic cleaning in an alkaline (pH = 9.7) detergent at 40°C, rinsing in cold demineralized water and finally drying in a hot air oven at 150°C.

5.2. Beam cleaning. In total three series of measurements were performed, studying the specific pressure rise $\Delta P/I$ as a function of the beam dose in mAh. The beam energy was 1.72 GeV throughout the measurements and the same test chamber was used with the synchrotron radiation always incident at 11 mrad glancing angle. During the three series of measurements the test chamber accumulated a total beam dose of 5900 mAh.

The first series of measurements were carried out on the test chamber after pumpdown from atmospheric pressure without bakeout. The test chamber had, however, been previously baked at 150°C for 20 h at CERN prior to mounting in the DCI machine as part of the leak checking and initial vacuum testing procedure.

The data of the first series were obtained during three runs with intervals of up to 3 weeks between each run and a total dose of 1600 mAh was accumulated. The specific partial pressure rise as a function of the DCI beam dose is shown in Figure 4. The four gases desorbed in order of importance were H_2, CO_2, CO and CH_4. The behaviour of H_2O, not shown in the figure, contrasted in that it did not appear to be desorbed. The H_2, CO and CO_2 more or less followed the same decrease with dose with an average slope of -0.7 and with no evidence of levelling off at high dose. The CH_4 decreased faster. The increase in desorption at 400 mAh dose was the result of leaving the chamber at 3×10^{-8} torr for 3 weeks between the second and third runs and resulted in an increase in desorption of all four gases. Evidence of a similar recontamination was observed over the 11 days separating the first and second runs at 31.6 mAh. The gap following 20 mAh was due to some additional measurements on the dependence of $\Delta P/I$ on angle of incidence where an estimated 11.6 mAh was accumulated by the test chamber.

It should be remembered that these results reflect the pumping speed for each individual gas species (see section 3.4, Table 1). A change in pumping speed for any one gas species will, of course, alter these figures. A presentation which is independent of the choice of the particular pumping speed is given in Figure 5 which

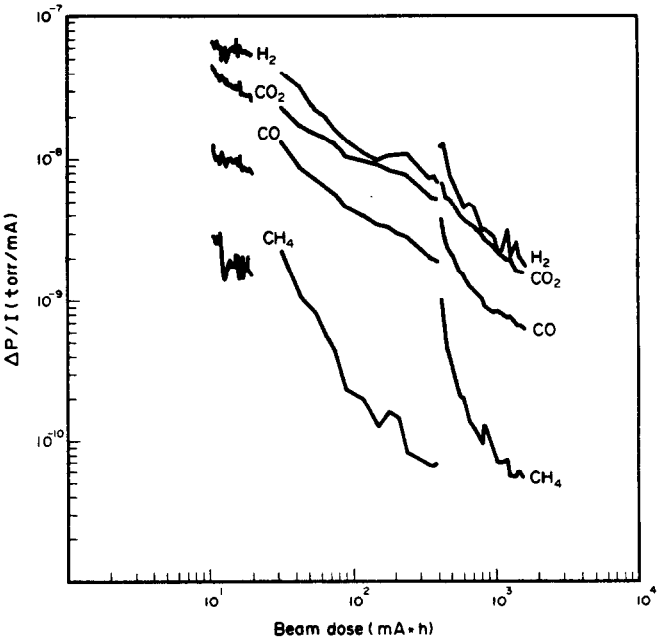

Figure 4. The specific partial pressure rise $\Delta P/I$ as a function of the beam dose for H_2, CH_4, CO and CO_2 for the first series of measurements—unbaked.

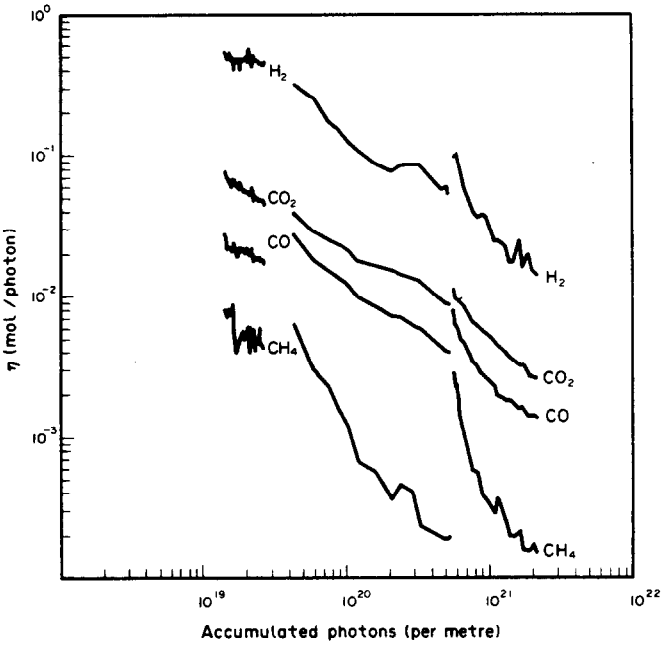

Figure 5. The molecular desorption yield η for H_2, CH_4, CO and CO_2 as a function of the accumulated number of photons for the first series of measurements—unbaked.

shows the same set of data as Figure 4 but after converting the specific pressure rise to molecular desorption yield η in molecules per photon. We have, furthermore, converted the beam dose in mAh at DCI to total number of photons per metre of test chamber as outlined in section 3.3 such as to present these results independent of the particular experimental configuration.

At the end of this first cleaning period we altered the test chamber position to measure the desorption from the opposite wall of the chamber, hence from a part of the surface which had so

far not been exposed to direct synchrotron radiation. The specific total pressure rise observed under this condition increased by a factor of approximately 2.2. The relatively small difference in desorption from the two opposite surfaces as compared to the achieved beam cleaning of more than one order of magnitude, shows that the synchrotron radiation cleans most of the inner surface of the vacuum chamber and not only the small region of primary incidence. This observation points to the importance of scattered photons and photoelectrons for the desorption process.

The second series of measurements were performed after venting the test chamber to the atmosphere followed by a 12 h bakeout at 150°C. The total beam dose accumulated during this series was 2000 mAh. The dose dependence of the specific pressure rise is shown in Figure 6. The recontamination at 1000 mAh

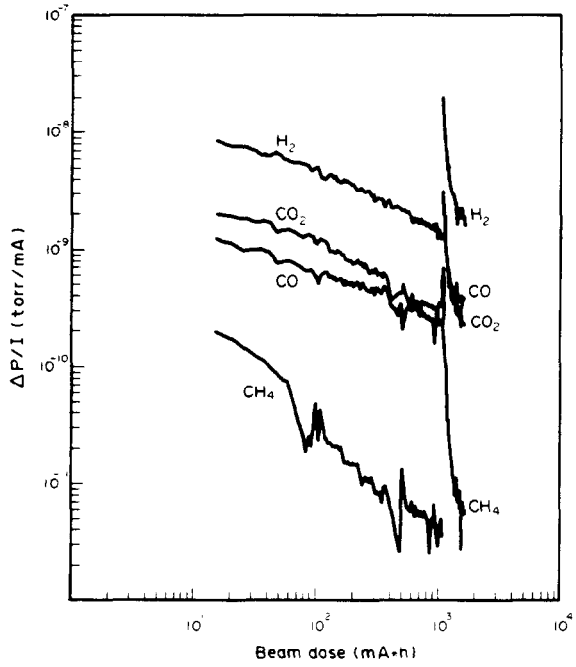

Figure 6. The specific partial pressure rise $\Delta P/I$ as a function of the beam dose for H_2, CH_4, CO and CO_2 for the second series of measurements—baked.

between the two runs of this series was due to a power cut which led to the ion pump remaining off for about 5 days. The recontamination resulted in an increase of all four gases. On the logarithmic plot the specific partial pressure rise for H_2 and CO_2 showed an increasing slope with dose. The CO showed a tendency to saturate with dose and the CH_4 cleaned up fastest of all. Once again the H_2O, not shown on the figure, did not desorb but rather slightly decreased with dose. Figure 7 shows the results converted to molecular desorption yield as function of the accumulated photons per metre. We observe that in this second experiment with the baked and re-exposed chamber the initial surface cleanliness had been improved by about a factor of 10 as compared to the first exposure of the unbaked test chamber. But the overall improvement in $\Delta P/I$ after the 2000 mAh of the second experiment is for H_2, CO and CO_2 less than a factor of 10 compared to the factor of about 30 during the 1600 mAh exposure of the first series.

The third series of measurements was preceded by a venting to air followed by pumpdown for about 1 week without bakeout. In

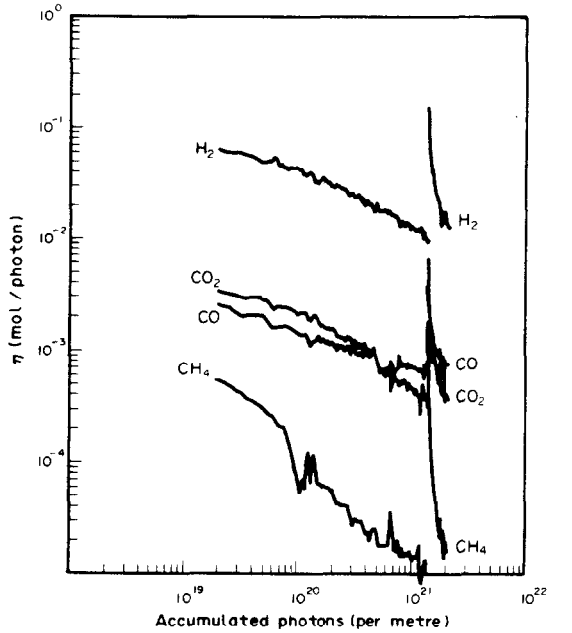

Figure 7. The molecular desorption yield η for H_2, CH_4, CO and CO_2 as a function of the accumulated number of photons for the second series of measurements—baked.

Figure 8 are shown the specific pressure increases as a function of DCI beam dose and in Figure 9 the molecular desorption yield as function of the total accumulated photons per metre for the third series of measurements. The two runs of this series were separated by a stop of only 12 h after a dose of about 1000 mAh and the resulting recontamination of all four gases can be seen. The step at 200 mAh was the result of stopping and continuing the measurement with a new higher intensity beam. The total beam dose of this series was 2300 mAh. This experiment represents a repetition

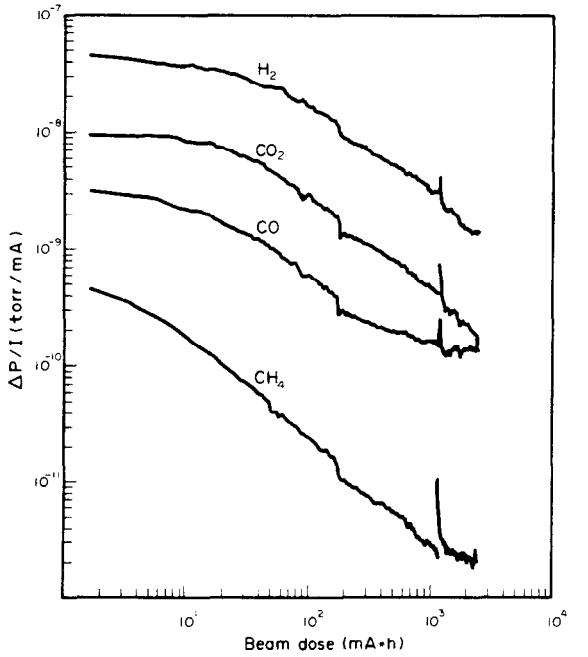

Figure 8. The specific partial pressure rise $\Delta P/I$ as a function of the beam dose for H_2, CH_4, CO and CO_2 for the third series of measurements—unbaked.

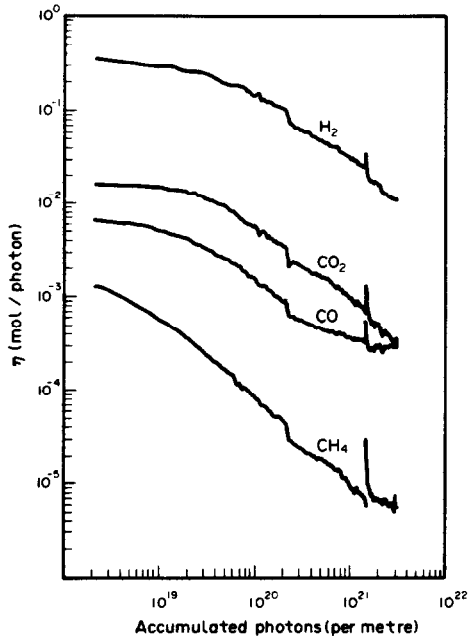

Figure 9. The molecular desorption yield η for H_2, CH_4, CO and CO_2 as a function of the accumulated number of photons for the third series of measurements—unbaked.

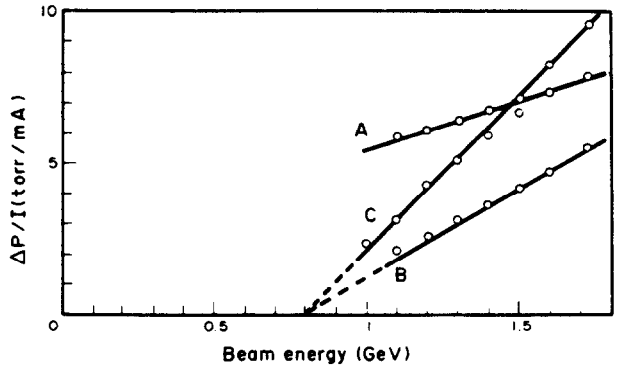

Figure 10. The dependence of the total specific pressure rise $\Delta P/I$ on beam energy.
Curve A: vertical scale $\times 10^{-9}$ torr mA^{-1}, perpendicular incidence, 10 mA h beam dose.
Curve B: vertical scale $\times 10^{-8}$ torr mA^{-1}, 11 mrad glancing angle of incidence, 10 mA h beam dose.
Curve C: vertical scale $\times 10^{-10}$ torr mA^{-1}, 11 mrad glancing angle of incidence, 2300 mA h beam dose.

of the first series of measurements on an unbaked system with the important difference, however, that the test chamber had already been cleaned twice in the preceding experiment. It was therefore important to establish the existence of a memory effect and its relative importance as compared to the total beam cleaning cycle.

It was observed that the total pressure decreased more slowly at first, this behaviour being reflected in the H_2 and CO_2 partial pressures. Once again, CO shows a reluctance to clean. The order of importance is still H_2, CO_2, CO and CH_4. When compared to the first series of measurements, a memory effect can be observed for the desorption of all gas species. This improvement in the initial surface cleanliness (at 10 mAh beam dose) amounts to factors of about 2 for H_2, 5 for CO and CO_2 and 10 for CH_4. Compared to the results of the second series of measurements the unbaked chamber shows a larger initial desorption by a factor of about 3 for H_2 and CO_2 while CO and CH_4 are essentially the same. This 2300 mAh dose resulted in an improvement of a factor of about 20 over the initial $\Delta P/I$ values.

5.3. Energy dependence. Figure 10 shows the energy dependence of the total specific pressure rise $\Delta P/I$ for perpendicular and for glancing incidence of the synchrotron radiation. Curves A and B were obtained on the newly installed test chamber which had been exposed to a total dose of only about 10 mA h. Curve C was obtained on the chamber which had undergone the 3 beam cleaning cycles and had received a dose of 2300 mAh since the last venting to air (i.e. at the end of the third series of measurements).

We find that the specific pressure rise is a linear function of energy in the range from 1 to 1.72 GeV. One notes that apart from the absolute scale which depends on dose, the extrapolation of curves B and C intercepts the energy axis at the same point of 0.8 GeV. Comparing curve A for perpendicular incidence with curves B and C it is seen that at the glancing angle of incidence the energy dependence of the specific pressure rise is stronger—between 1.1 and 1.72 GeV the value of $\Delta P/I$ increases by a factor of about 3 as compared to 1.3 for curve A.

The observations are at least in qualitative agreement with a desorption model which assumes that the interaction leading to desorption only takes place in the surface layer and that high energy photons which are able to penetrate deeper into the bulk are ineffective. Increasing the beam energy yields a photon spectrum which extends to higher energies but which is essentially unchanged for photon energies below the critical energy (which is 300 eV at 0.8 GeV, 790 eV at 1.1 GeV and 3 keV at 1.72 GeV). The observed behaviour would therefore suggest that as the glancing angle of incidence of the photons is decreased, the interaction of the photons occurs closer to the surface and consequently the desorption by the high energy part of the photon spectrum becomes more and more important.

We may therefore express the specific pressure rise as

$$\Delta P/I = K(E - E_c)$$

where the constant K depends on the accumulated beam dose and E_c is an apparent threshold or cut-off energy which appears to be independent of beam dose for a given angle of incidence. The dependence of E_c on the angle of incidence (see curve A) has yet to be studied. For 11 mrad angle of incidence we find $E_c = 0.8$ GeV in DCI. Scaled to LEP E_c would have to be multiplied by the factor of 9.33 which accounts for the different beam energy at the same photon spectrum. The corresponding cut-off energy in LEP would therefore be expected to be at 7.5 GeV.

5.4. Angle of incidence dependence. The observed dependence of the specific pressure rise on the angle of incidence at constant beam energy of 1.72 GeV is shown on Figure 11. The measurement was performed on the new chamber after an accumulated dose of 20 mA h.

Our experimental results are not in agreement with the $1/\sin\phi$ dependence which has frequently been assumed in the past for scaling desorption rates to glancing angle incidence[4]. Indeed, for the situation in LEP the expected effect of the angle will be less than a factor of 10 as compared to the factor of more than 150 implied by the inverse sine law. Because of lack of time this measurement could not be repeated at another energy.

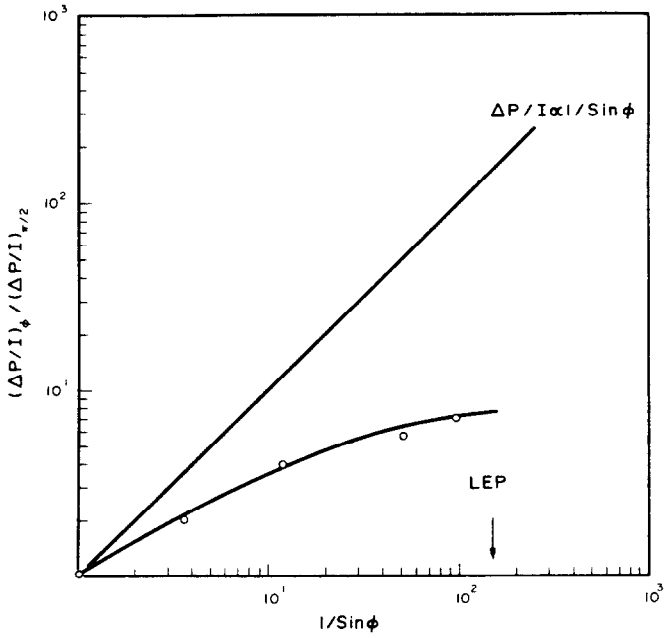

Figure 11. The dependence of the total specific pressure rise on the glancing angle of incidence at a beam energy of 1.72 GeV.

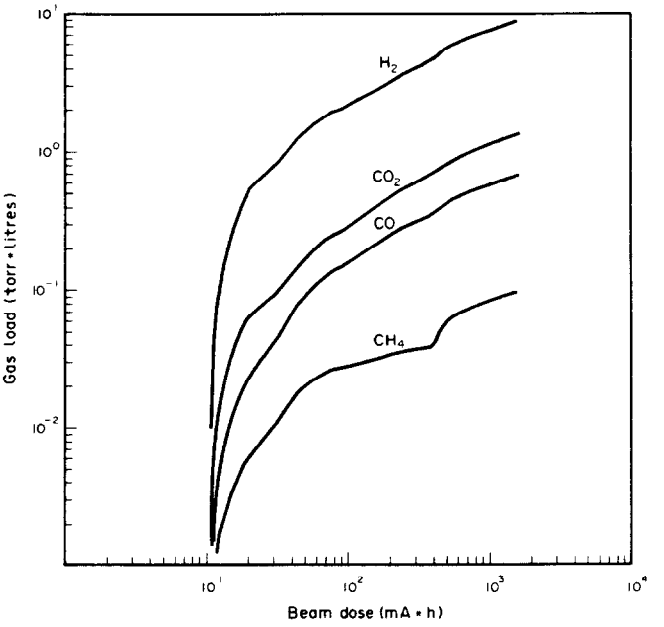

Figure 12. The total quantity of each gas species desorbed—the gas load—as a function of the beam dose for the first series of measurements—unbaked.

5.5. Integrated gas load. For the three series of measurements the total amount of gas desorbed from the chamber both thermally—static outgassing—and by the synchrotron radiation and pumped via the conductance was calculated and the resulting gas loads are shown in Figures 12, 13 and 14.

For comparison the integrated gas load during the first 500 mAh of the second and third series of measurements is summarized in Table 2, together with the value of the total specific pressure rise at that instant. In addition, the number of monolayers desorbed, θ_i, is given in the table. (The surface area of the test chamber per metre is 3300 cm^2, hence 1 torr l m^{-1} corresponds to the desorption of 10^{16} molecules cm^{-2}; for any of the five gases in Table 2 it is assumed that a monolayer contains 6.7×10^{14} molecules cm^{-2}.)

The important difference between the baked and the unbaked system appears to be the increased amount of hydrogen and water vapour in the unbaked situation. We have seen that water vapour as such does not contribute to the dynamic pressure rise but it may strongly affect the static base pressure in the system. In fact, for the baked case the amount of H_2O is certainly pessimistic since, as was explained in section 4.2 an abnormally high base pressure with a high H_2O content was obtained after bakeout due to a high thermal outgassing from the viton O-ring sealed valve. The beam dose of 500 mAh yields an average reduction in the desorption

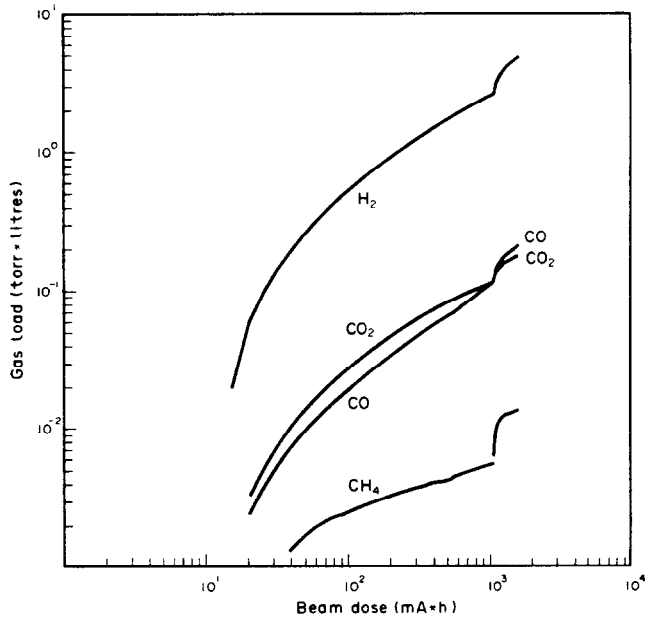

Figure 13. The total quantity of each gas species desorbed—the gas load—as a function of the beam dose for the second series of measurements—baked.

Table 2. Total specific pressure rise $\Delta P/I$, integrated gas load Q_i and number of monolayers desorbed θ_i after a beam dose of 500 mA h in DCI

	Baked system (2nd series) 3.5×10^{-9} torr mA^{-1}		Unbaked system (3rd series) 6.3×10^{-9} torr mA^{-1}	
$\Delta P/I$ total	Q_i (torr l m^{-1})	θ_i	Q_i (torr l m^{-1})	θ_i
H_2	0.614	9.2	1.51	22.5
CH_4	1.6×10^{-3}	2.4×10^{-2}	1.38×10^{-3}	2.1×10^{-2}
H_2O	6.5×10^{-4}	9.7×10^{-3}	6.0×10^{-3}	9.0×10^{-2}
CO	2.8×10^{-2}	4.2×10^{-1}	2.37×10^{-2}	3.5×10^{-1}
CO_2	2.9×10^{-2}	4.3×10^{-1}	6.8×10^{-2}	1

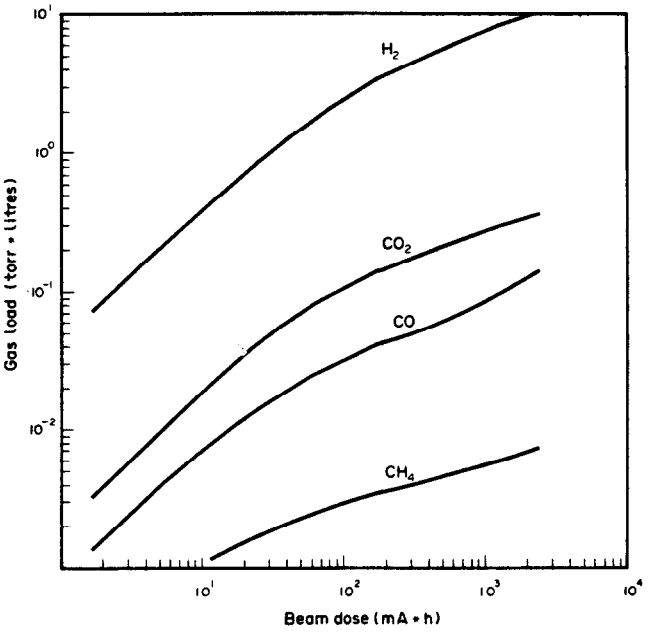

Figure 14. The total quantity of each gas species desorbed—the gas load—as a function of the beam dose for the third series of measurements—unbaked.

rates by roughly one order of magnitude. Much more H_2 than any other gas is desorbed. From the unbaked chamber, after a dose of 500 mAh, 22.5 monolayers are desorbed compared with 9.2 for the baked case. At the other extreme only 2.1×10^{-2} monolayers of CH_4 are desorbed from the unbaked chamber and 2.4×10^{-2} monolayers from the baked chamber. After 1000 mAh all these numbers have almost doubled and are still increasing. These figures, of course, do not give any information about the reservoir of undesorbed gas still on the surface and which may still be available for desorption.

The figure of 22.5 monolayers may appear to be somewhat high but the real surface area of the chamber, as opposed to the geometrical surface area, has to be taken into account. For example on 316 L + N stainless steel the real surface area can be as much as 14 times the geometric surface area[5] and such a high so-called roughness factor for our Al alloy surface cannot be excluded. Measurements of the roughness factor for our chamber material are in progress and will be reported on later.

6. Beam lifetime

The effect the residual pressure will have on the lifetime of the circulating electron or positron beam in LEP has been evaluated elsewhere[6]. The theoretical beam-gas lifetimes, K_i, of the following gases are

H_2 53.5×10^{-8} torr h
CH_4 6.6×10^{-8} torr h
CO 3.4×10^{-8} torr h
CO_2 2.1×10^{-8} torr h.

These values depend only weakly on the particular machine parameters and may therefore be used to estimate the beam lifetime in machines different from LEP. Based on these figures we have analysed the three series of measurements in terms of the beam gas lifetime corresponding to the pressure and gas composition in the test chamber. The results shown in Figure 15 are presented in terms of the product $I\tau$, beam current and beam lifetime. They were obtained by summing the contributions of the different partial pressures,

$$I\tau = \left(\sum\left(\frac{1}{K_i} \cdot \frac{\Delta P_i}{I}\right)\right)^{-1}$$

but neglecting the contribution of the static pressure. The curves for the three measurements can be used to determine the beam cleaning dose required for a desired value of $I\tau$. Alternatively, if the beam current and the lifetime and hence the value of $I\tau$ are specified, Figure 15 gives the required beam dose. It should be noted that in order to apply these curves obtained at DCI to LEP it is necessary to use the scaling factor as derived in section 3.2, i.e. both horizontal and vertical scales have to be divided by 2.5. Furthermore, any change in pumping speed has to be properly taken into account.

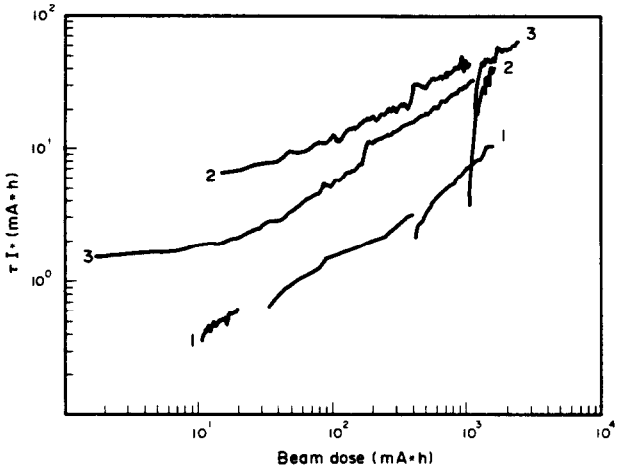

Figure 15. The product of beam lifetime τ and circulating beam current I as a function of beam dose for the three series of measurements.

7. Summary

In this report we have summarized the results of vacuum measurements on a prototype section of the LEP vacuum chamber exposed to synchrotron radiation emerging from the DCI storage ring. An attempt has been made to simulate the conditions expected in LEP as closely as possible. For this reason, the running conditions of DCI were chosen near its top energy to obtain a photon spectrum similar to LEP at injection energy. The critical energies of the photon spectra are 3 keV and 6 keV for DCI and LEP respectively. In addition, the glancing angle of incidence of the synchrotron radiation was chosen to be as close as possible to the 6 mrad in LEP but for practical reasons was limited to 11 mrad. The execution of the experiment benefited greatly from the fact that due to the high current capability of DCI a given beam dose in terms of mA h could be accumulated in a short time. However, in the case where beam cleaning depends on the photon flux, then our results may have to be corrected for this effect.

Here, we have made no attempt to interpret the results in terms of direct photon desorption or of a two stage process involving the production of photoelectrons. In subsequent measurements at DCI this question has been studied in more detail by measuring the photoelectron current in the test chamber and the results will

be presented in a future publication. Our global results on the clean-up rate on exposure to synchrotron radiation are in agreement with previous experience from the DCI main ring and with observations on other storage rings[7]. Also, attention has to be drawn to the fact that contrary to the situation in a storage ring, our test chamber was not in a magnetic field. We cannot exclude that the absence of a magnetic field influences the clean-up behaviour.

In order of importance the gases desorbed were H_2, CO_2, CO and CH_4. Here it is interesting to note that CH_4 which could become a critical gas component in a predominantly getter pumped system, appears to decrease as a function of beam dose with at least the same rate as the other active gases. There is furthermore some evidence that this gas species shows an accumulative cleaning effect during the three successive cycles of measurements. Despite being in the residual gas phase H_2O did not appear to be desorbed but if anything decreased during photon bombardment.

Throughout the experiment we worked with the same chamber section. For this reason the interesting aspect of the memory effect of a cleaned chamber after exposure to air and the benefit of a bakeout on the initial desorption cannot be fully separated. Comparing the initial desorption rates (at 10 mA h) of the first and of the third series of measurements we find an improvement of between 2 and 10 for the various gas species.

The observations of the dependence of the specific pressure rise on the angle of incidence suggest that this effect is indeed much weaker than the frequently used scaling which the inverse sin law would indicate. In addition, we have also evidence that the angular dependence is a function of the energy of the photons. It will therefore be important to continue the so far only preliminary measurements in order to arrive at a better scaling for the conditions in LEP.

A comparison of the dependence of the specific pressure rise at perpendicular incidence with the one for glancing incidence leads to the conclusion that at glancing incidence the contribution of the low energy photons in the spectrum to the desorption is of a reduced importance.

On the contrary, at perpendicular incidence the low energy photons in the spectrum appear to produce the main part of the desorption. A better understanding of these energy and angle related effects could be helpful to assess the importance of the photoelectron induced desorption relative to the direct photodesorption process as mentioned before.

Inspection of Figure 15 leads to the conclusion that for the initial operation of LEP acceptable beam lifetimes of several hours may be obtained after a beam cleaning period of several hundred mA h. For a chamber which had already been exposed to synchrotron radiation, then vented to the atmosphere and repumped the same beam lifetime can be obtained after a beam dose of about a factor of 10 less.

Acknowledgements

The authors wish to thank Prof J. Perez y Jorba for his support of this work and for providing the necessary machine time on DCI. Dr P Marin is thanked for his continual encouragement and useful discussions. The expertise of the DCI operations crew is also gratefully acknowledged and the very competent assistance provided by Mr H Mozian in the installation and operation of the experiment is much appreciated. The technical assistance of Mr C Flament of the ISR General Engineering Group has been of great value during the course of the work.

References

[1] CERN Report, CERN/ISR-LEP/79-33, 22 August 1979.
[2] A A Sokolov and I M Ternov. *Synchrotron Radiation.* Pergamon Press Ltd., Oxford (1968).
[3] R A Mack, Spectral and Angular Distributions of Synchrotron Radiation, CEAL-1027, February 1966.
[4] J Kouptsidis and A G Mathewson, DESY 76/49 (1976).
[5] K Watanabe, S Maeda, T Yamashina and A G Mathewson. *J Nucl Mater*, **93 and 94**, 679 (1980).
[6] H Störi, *Vacuum*, **33**, 171 (1983).
[7] C H Falland *et al.*, *Proc 8th Int Vacuum Congress*, p 126, Cannes, 1980.